Original Article

Proteomic profiles and cytokeratin 13 as a potential biomarker of Ovis aries Papillomavirus 3-positive and negative cutaneous squamous cell carcinomas

Veronica Vitiello[a#], Giovanni P. Burrai[a,b*#], Salvatore Pisanu[c], Carla Cacciotto[a,b,c], Maria Filippa Addis[b,c,d], Alberto Alberti[a,b], Elisabetta Antuofermo[a,b], Tiziana Cubeddu[a,b], Salvatore Pirino[a]

[a] *Department of Veterinary Medicine, University of Sassari, Via Vienna 2, 07100, Sassari, Italy.*
[b] *Mediterranean Center for Disease Control, University of Sassari, Via Vienna 2, 07100, Sassari, Italy.*
[c] *Porto Conte Ricerche Srl, S.P. 55 Porto Conte/Capo Caccia Km 8.400, Tramariglio, 07041 Alghero (SS), Italy.*
[d] *Department of Veterinary Medicine, University of Milan, Via Celoria 10, 20133, Milan, Italy.*

*Corresponding Author: Telephone: +39079229440, *E-mail address*: gburrai@uniss.it (GP. Burrai)

[#]These authors contributed equally to this work

Abstract

Ovis aries papillomavirus 3 (OaPV3) is an epidermotropic PV reported in sheep cutaneous squamous cell carcinoma (SCC). The presence of OaPV3 DNA and its transcriptional activity in cutaneous SCC, as well as its *in vitro* transforming properties, suggest a viral etiology for this neoplasm. Nevertheless, the reactome associated with viral-host interaction is still unexplored.

Here, we investigated and compared the proteomic profiles of OaPV3-positive SCCs, OaPV3-negative SCCs, and non-SCC samples by liquid chromatography tandem-mass spectrometry (LC-MS/MS) analysis, bioinformatics tools, and immunohistochemistry (IHC). OaPV3-positive SCCs (n = 3), OaPV3-negative SCCs (n = 3), and non-SCCs samples (n = 3) were subjected to a shotgun proteomic analysis workflow to assess protein abundance differences among the three sample classes. Proteins involved in epithelial cell differentiation, extracellular matrix organization, and apoptotic signaling showed different abundances in OaPV3-positive SCCs tissues ($P \leq 0.05$) when compared to the other tissues. Cytokeratin 13 (CK 13) was among the most increased proteins in OaPV3-positive SCC and was validated by immunohistochemistry on 10 samples per class, confirming its potential as a biomarker of OaPV3 infection in SCC.

Collectively, results provide a preliminary insight into the reactome associated with viral-host interaction and pave the way to the development of specific biomarkers for viral-induced sheep SCC.

Keywords: Cytokeratin 13, papillomavirus, sheep, squamous cell carcinoma, reactome

Introduction

Squamous cell carcinoma (SCC) is a malignant tumor arising from the squamous epithelium of the skin and mucous membranes, widely reported in domestic animals and represents the most common form of skin tumor in sheep (Alberti et al., 2010; Tore et al., 2017; Vitiello et al., 2017; Goldschmidt et al., 2017).

Papillomavirus infection, along with several environmental risk factors, such as prolonged exposure to ultraviolet radiation of poorly pigmented skin, has been claimed to act as a major factor contributing to SCC development (Alberti et al., 2010; Ahmed et al., 2015). PVs are a large group of small, non-enveloped, double-stranded DNA viruses that infect skin and mucosae causing proliferative and neoplastic lesions in domestic and wild vertebrate species (Munday et al., 2010; Lange et al., 2011; Rector et al., 2013; Sardon et al., 2015; de Villiers et al., 2017; Lecis et al., 2020).

In sheep, four PV types, namely Ovis aries Papillomavirus 1 (OaPV1), 2 (OaPV2), 3 (OaPV3), and 4 (OaPV4), have been fully sequenced and classified into two different genera (Alberti et al., 2010; Tore et al., 2017). OaPV1, OaPV2, and OaPV4 have been rescued from cutaneous fibropapillomas and belong to the *Delta* genus, while OaPV3 has been detected in cutaneous SCC and is the prototype of the *Dyokappa* genus (Alberti et al., 2010; Tore et al., 2017). Although the putative etiological role of *ovine PVs* both in cutaneous fibropapilloma and SCC has not yet been fully elucidated, it has been shown that OaPV3 expresses the typical E6/E7 oncogenes, and that OaPV3 E7 binds the retinoblastoma tumor suppressor protein (pRb) much more efficiently than fibropapilloma-related papillomaviruses, similarl to what has been observed in high and low - risk human PVs (Alberti et al., 2010; Tore et al., 2019). Additionally, the presence of both OaPV3 DNA and transcripts in SCCs, as well as its in vitro transforming properties, point towards a contribution of OaPV3 to tumor development (Alberti et al., 2010; Vitiello et al., 2017; Tore et al., 2019).

Proteomic profiling technologies open the way to the discovery of novel biomarkers with potential as sensitive and specific molecular tools in cancer research (Mabert et al., 2014). The identification of altered proteins occurring in the oncogenesis process, as well as their qualitative and quantitative characterization, can offer valuable information relating to more effective diagnosis, prognosis, and response to therapy. Thus, the application of proteomics to ovine SCC appears particularly interesting in order to map the biological processes associated with viral infection, in which OaPV3 could play a pivotal role. Furthermore, characterizing the proteins involved in virus-host interactions can contribute to the identification of candidate biomarkers indicating viral activity. Based on these considerations, the aim of our study was to discover and validate OaPV3 infection-related proteins in ovine cutaneous SCC by proteomics and immunohistochemistry (IHC), in order to elucidate the pathways involved in viral neoplastic transformation and to identify potential viral biomarkers.

Materials and Methods

Origin of the samples

This study included a total of 30 archival tissue samples, of which 10 were OaPV3-positive SCCs, 10 were OaPV3-negative SCCs, and 10 were non-SCC samples collected from the udder (n = 17) and the head (n = 13) of 30 Sarda breed sheep. All tissues belonged to a previous sampling study (Vitiello et al., 2017) in which specimens were divided in two aliquots, one of which was formalin-fixed, paraffin-embedded (FFPE), and used for histological evaluation and immunohistochemistry, while the other was frozen at -80°C for later proteomic analyses. In that study (Vitiello et al., 2017) the presence of OaPV3 in sheep SCC was assessed by conventional PCR, and its cellular localization and transcriptional activity were evaluated by ISH and RT-PCR. All SCCs were classified as moderately differentiated (except 1 classified as poorly differentiated) according to the

96 modified Anneroth's multifactorial histological grading system by two experienced (EA, SP) and
97 one board-certified pathologist (GPB) (Vitiello et al., 2017).
98 Experiment permission was not required from the University's Animal Care Ethics
99 Committee because all the samples were retrieved from the abattoir.
100
101 *Protein extraction, in-gel digestion, shotgun analysis, and protein identification*
102 For proteomic analysis, frozen udder tissue samples from 3 moderately differentiated
103 OaPV3-positive SCCs, 3 moderately differentiated OaPV3-negative SCCs, and 3 non-SCCs were
104 selected among the 30 archival samples listed in the previous paragraph and characterized in our
105 previous study (Vitiello et al., 2017). For protein extraction, the tissue replicates stored at -80°C
106 were included in Optimal Cutting Temperature medium (Tissue-Tek, Sakura Finetek, Torrance,
107 CA, USA), cut into 20 serial cryosections (Leica CM 1950, Heidelberg, Germany) at 10-µm, and
108 collected in a 1.5-ml sterile tube. In parallel, serial cryostat sections (3-µm thick) from the same
109 tissue were histologically evaluated in order to confirm their classification and to ensure that the
110 lesions were present in the portion of the tissue subjected to proteomic analysis, as well as to re-
111 assess non-SCC tissues. Total proteins were extracted from each tissue by incubating the respective
112 10-µm cryosections in 200 µl of lysis buffer containing 2% sodium dodecyl sulphate (SDS), 0.4 %
113 Tween-20, 130 mM dithiothreitol (DTT), 500 mM Tris HCl (pH 8.8) plus SIGMAFAST™ Protease
114 Inhibitors (Sigma, St. Louis, MO, USA) at the concentration recommended by the manufacturers, at
115 300 rpm for 15 min at 95 °C using a Thermomixer comfort (Eppendorf, Hamburg, Germany). After
116 centrifugation at 10.000 x g for 10 min at 4° C, supernatants were quantified with the PierceTM 660
117 nm Protein Assay (Thermo Scientific). Protein extracts were processed to obtain peptide mixtures
118 by means of the Filter Aided Sample Preparation (FASP) as previously described, starting from 100
119 µg of protein extract (Wisniewski et al., 2009; Tanca et al., 2013). Then, liquid chromatography-
120 tandem mass spectrometry (LC-MS/MS) analysis of tryptic digests was performed on a Q-TOF
121 hybrid mass spectrometer with a nano lock Z spray source, coupled on-line with a NanoAcquity

chromatography system (Waters). Each peptide mixture was analyzed in duplicate and each sample was first concentrated, washed with an enrichment column, fractionated over a 250 min gradient on a C18 reverse-phase column and then analyzed by a data-dependent MS/MS mode as described previously (Ghisaura et al., 2019). Raw files were processed by ProteinLynx software (Version 2.2.5) to produce the peak lists as pkl files. All pkl files were first converted into MGF files, and subsequently, Proteome Discoverer software (version 1.4; Thermo Scientific) was used for protein identification. Two technical replicates were analyzed as merge to generate a unique list of proteins for each biological sample using a workflow assembling by different nodes: Sequest-HT as a search engine (Protein Database: database homemade composed by concatenation of different databases obtained by UniProtKB; Taxonomy: *Bos taurus*, *Ovis aries* and *Capra hircus* sequences from SwissProt and Papillomaviridae sequences from TrEMBL; Enzyme: Trypsin; Maximum missed cleavage sites: 2; Precursor mass tolerance: 50 ppm; Fragment mass tolerance: 0.4 Da; Static modification: cysteine carbamidomethylation; Dynamic modification: N-terminal Glutamine conversion to Pyro-glutamic acid and methionine oxidation), and Percolator for peptide validation (peptide confidence: q-value < 0.01) (Kall et al., 2007; The et al., 2016). Peptide and protein grouping according to the Proteome Discoverer's algorithm were allowed, applying the strict maximum parsimony principle.

Label-free quantitation and data analysis

Spectral counts (SpC) were used to estimate protein abundances and to compare the abundance of the same proteins between different sample groups (Addis et al., 2011; Pisanu et al., 2011; Tanca et al., 2013). The Normalized Spectral Abundance Factor (NSAF) of proteins was used to express their relative abundance and the SpC log Ratio (R_{SC}) to express the log fold change of proteins between different experimental groups (Old et al., 2005; Zybailov et al., 2006). Proteins identified with less than one SpC in at least one replicate or with fewer than two SpCs in more than one replicate were excluded from the differential analysis, in order to increase the accuracy of the

148 analysis (Addis et al., 2011; Addis et al., 2013). Among proteins identified in the databases of *Bos*
149 *taurus*, *Ovis aries,* and *Capra hircus* proteins, only those with the highest number of peptides and
150 PSMs were considered.
151
152 *Functional analysis of differential proteins*
153 All proteins showing statistically significant differences in OaPV3-positive SCCs, OaPV3-negative
154 SCCs, and non-SCC tissues were subjected to pathway analysis based on the Gene Ontology (GO)
155 database (biological processes (BP), molecular functions (MF), and cellular components (CC)) and
156 STRING (Szklarczyk et al., 2015; Pisanu et al., 2018). To enable pathway analysis, the UniProt
157 codes for *Bos taurus*, *Ovis aries,* and *Capra hircus* were replaced with the UniProt codes for the
158 closest human protein equivalent by sequence alignment of identified peptides with human
159 sequences using Basic Local Alignment Search Tool (BLAST).
160
161 *Immunohistochemistry*
162 Histological sections (3-µm thick) of the 30 FFPE samples described in the first paragraph
163 (OaPV3-positive SCCs, OaPV3-negative SCCs, non-SCC samples, 10 samples per class,
164 respectively), were mounted on charged slides (Superfrost Ultra Plus, Thermo Scientific), as
165 previously described (Banco et al., 2011). Briefly, slides were immersed for 20 min in a 98°C
166 preheated solution (WCAP, BioOptica, Milan, Italy) and mounted in a sequenza chamber (Shandon,
167 Runcorn, UK). Tissues were then blocked for endogenous peroxidase with a 1 h incubation in Dako
168 REAL Peroxidase-Blocking Solution (S2023, Dako, Glostrup, Denmark), and for non-specific
169 binding with a 1 h incubation in 2.5% normal horse serum (ImmPRESS reagent kit, Vector Labs,
170 Burlingame, CA, USA). Subsequently, slides were incubated overnight at 4°C with rabbit
171 polyclonal antibodies against CK 13 (ab58744, ABcam, Cambridge, UK) at 1:400. Next, slides
172 were incubated for 30 min at room temperature with an anti-rabbit secondary antibody (ImmPRESS
173 reagent kit, Vector Labs, Burlingame, CA, USA). After staining with 3,3'-Diaminobenzidine

(ImmPACT DAB, Vector Laboratories, Burlingame, CA, USA) tissues were counterstained with hematoxylin, cover-slipped with Eukitt Mounting MediumTM (BiOptica, Milan, Italy) and observed under light microscopy. Urinary bladder tissue sections were used as positive controls for CK 13. Negative controls were carried out by replacing the primary antibody with normal rabbit serum (Invitrogen, Milan, Italy).

Evaluation of immunohistochemical data

The extent of CK 13 immunopositivity was evaluated by considering the cytoplasmic signals of the malignant squamous cells or non-neoplastic skin cells. Immunoreactivity was semi-quantitatively scored considering the number of positive cells in 10 HPF (grade 0: no positive cells; 1: < 10%; 2: 11-30%; 3: 31-60%; 4: > 60%) and the intensity of staining (weak: 1; moderate: 2; strong: 3). Then, a combined immunoreactivity score (IRS) ranging from 1 to 12 was calculated for each specimen. Tissues were imaged using Nikon Eclipse 80i and digital computer images were recorded with a Nikon Ds-fi1 camera.

Statistical analysis

All the statistical analyses, including descriptive statistics, were performed using Stata 11.2 software (StataCorp LP), with statistical significance set as $P \leq 0.05$. To evaluate differentially abundant proteins (Rsc) among the experimental groups, we applied the beta-binomial test (Pham et al., 2010). Only proteins with $Rsc \geq 1.5$ or ≤ -1.5 and with a P-value ≤ 0.05 obtained by the beta-binomial test were considered significant in the comparison between OaPV3-positive SCCs, OaPV3-negative SCCs, and non-SCC samples. To evaluate the differences between the principal biological processes obtained by STRING, we used NSAF values and Student t-test after checking the normality with the Shapiro-Wilk test. Abundances of the different biological processes were calculated by the sum of the NSAF values for each protein associated to a biological process (Addis et al., 2011).

Results

Proteomic analysis of SCC and non-SCC sheep tissue samples

A total of 476 proteins were successfully identified (Sheet 1 "1. All identified proteins", Supplementary File). Of these, 242 were eligible for the differential analysis between OaPV3-positive SCCs, OaPV3-negative SCCs, and non-SCC tissues, by label-free quantitative proteomics. Differential proteomics results are reported in Table 1.

Differential proteins between OaPV3-positive SCCs and OaPV3-negative SCCs

A total of 28 proteins showed statistically significant differences (Rsc ≥ 1.5 and ≤-1.5, *P*-value ≤ 0.05) when comparing OaPV3-positive with OaPV3-negative SCCs. Of these, 17 proteins were increased and 11 were decreased (Table 1, OaPV3 vs SCC, in bold; Sheet 2 "2. Pos SCCs vs Negative SCCs", Supplementary File).

Differential proteins between OaPV3-positive SCCs and non-SCC tissues

A total of 43 proteins showed statistically significant differences (1 Rsc ≥ 1.5 and ≤-1.5, P-value ≤ 0.05) when comparing OaPV3-positive SCCs with non-SCC tissues. Of these, 14 proteins were increased while 29 were decreased (Table 1, OaPV3 vs N, in bold; Sheet 3 "3. Pos SCCs vs non-SCC tissue", Supplementary File).

Differential proteins between OaPV3-negative SCCs and non-SCC tissues

A total of 26 proteins showed statistically significant differences (Rsc ≥ 1.5 and ≤-1.5, *P*-value ≤ 0.05) when comparing OaPV3-negative SCCs with non-SCC tissues. Of these, 7 proteins were increased and 19 were decreased (Table 1, SCC vs N, in bold; Sheet 4 "4. Neg SCCs vs non-SCC tissue", Supplementary File).

Biological and functional pathways involving differential proteins

The proteins showing statistically significant changes belonged to numerous biological pathways related to the disease. The most relevant ones were response to stress (RS, 28 proteins), regulation of apoptotic signalling pathways (RASP, 7 proteins), negative regulation of apoptotic process and cell death (NRAP, 10 proteins), tissue development (TD, 18 proteins), epithelial cell differentiation (ECD, 8 proteins), extracellular matrix disassembly (EMD, 5 proteins) and organization (EMO, 9 proteins), and glycosaminoglycan catabolic process (GCP, 4 proteins). Differential proteins belonging to these pathways and significant in at least one sample group (bold type) are indicated in Table 1 with asterisks in each respective pathway column. Detailed information is reported in Supplementary File, Sheet 5 "5. Biological Process_STRING" and sheet 6 "6. Table with Gene Ontology".

The biological pathways most represented in each SCC type and in non-SCC tissues were then assessed by considering the total abundance of all the proteins belonging to each pathway within the different sample groups (Fig.1). As a result, OaPV3-positive SCCs had a significantly higher abundance of proteins belonging to the functional classes RASP, NRAP, and NRCD when compared to both OaPV3-negative SCC and non-SCC tissues. OaPV3-positive SCCs also contained higher amounts of proteins belonging to the functional class RS when compared to non-SCC tissues. On the other hand, OaPV3-positive SCCs had lower amounts of proteins belonging to TD and ECD when compared to both OaPV3-negative SCC and non-SCC tissues. OaPV3-positive SCCs did also have lower amounts of proteins belonging to EMD and EMO when compared to non-SCC tissues. The proteins participating in each pathway are indicated in Table 1 with the respective abbreviations, and are detailed in the Supplementary file, Sheet 5 "Biological Process_STRING". Protein abundance values are detailed in Sheet 7 "7.NSAF".

Reactome analysis was also carried out on all differential proteins to highlight common pathways involved in the development of SCC. The resulting protein network is reported in Fig. 2.

The most significantly represented pathway was “neutrophil degranulation”, followed by “innate immune system”. Of interest in the context of the disease was the significant involvement of “formation of the cornified envelope”, “degradation of the extracellular matrix”, as well as “Chk1/Chk2(Cds1) mediated inactivation of “Cyclin B:Cdk1 complex”. Results are detailed in Sheet 8 “8. Reactome_STRING”, Supplementary file.

Immunohistochemistry

Among differentially expressed proteins, CK 13 was higher in OaPV3-positive SCCs when compared to either OaPV3-negative SCCs or non-SCC tissues, in both cases with high RSC values. To validate this observation, CK 13 abundance in the 3 sample classes was further investigated by IHC on a larger cohort (10 samples for each class) (Fig. 3). As a result, 10/10 OaPV3-positive SCCs (100%) showed diffuse and strong cytoplasmic CK 13 signals in the intermediate and superficial layers of malignant squamous cells, with rare signals in the epithelial basal layer. Specifically, 6/10 OaPV3-positive SCCs (60%) showed a strongly immunoreactive signal (IRS score = 12) (Fig. 3a), whereas 4/10 (40%) showed weak immunostaining (IRS score = 4) (Fig. 3b). Only 2 out of 10 OaPV3-negative SCCs (20%) showed a barely detectable signal in suprabasal cells (IRS score = 2), while no signal was detected in 8/10 OaPV3-negative SCC (80%, IRS score = 0) (Fig. 3c) and in 10/10 non-SCC samples (100%, IRS score = 0). Strong immunoreactivity was detected in the cytoplasm of the bladder epithelial cells used as positive controls, while no signal was observed in the negative controls.

Discussion

Proteomic analysis appears particularly interesting in cancer research, as both the study of tumor cell biology and the identification of altered cellular processes and of the specific proteins involved in these pathways represent key tools for investigating tumors (Srivastava et al., 2018). Investigating the reactome of diseased animals does also provide new insights in veterinary

medicine, helping to clarify molecular mechanisms dictating initiation and progression of different conditions, and allowing the identification of specific biomarkers that may be useful for establishing effective intervention and treatment control actions (Ceciliani et al., 2014; Lippolis et al., 2016).

Accordingly, when looking at the functional pathways involving the differential proteins identified in this study and at their reactome, a significantly higher abundance of proteins belonging to regulation of apoptotic signalling pathways, negative regulation of apoptotic process, and negative regulation of cell death, was found in OaPV3-positive SCC. These pathways are involved in SCC development and were related to the presence or absence of OaPV3 infection. On the other hand, other pathways associated with normal tissue and extracellular matrix organization were more abundant in non-SCC tissues, followed by OaPV3-negative SCC.

When investigating the reactome, the most significantly altered pathways in the investigated SCC tissues were related to neutrophil degranulation and the innate immune system as well as platelet degranulation and activation and, more in general, to the hemostasis system. It seems plausible that this might be related to the inflammatory reaction due to the high frequency of SCC ulceration, as observed in our cases, and frequently described also in goats (Gibbons et al., 2015). Furthermore, the role of tumor-associated neutrophils (TANs) has gained attention in cancer and has been linked to the overall survival of human patients with both oesophageal and head and neck squamous cell carcinoma (Shaul et al., 2019).

Concerning differential proteins, several were involved in SCC development and were related to the presence or absence of OaPV3 infection. Among proteins significantly higher in OaPV3-positive SCCs when compared to non-neoplastic samples, transgelin-2, annexin, pyruvate kinase, alpha-1-acid glycoprotein have been reported as key factors for the progression of human SCC (Croce et al., 2001; Calmon et al., 2013; Meng et al., 2017; Kurihara-Shimomura et al., 2018). Also, previous studies reported Annexin A1 overexpression in penile carcinomas positive for high-risk HPVs (Calmon et al., 2013).

Additionally, 14-3-3 proteins theta and zeta/delta (Table 1) were more abundant in SCCs harboring OaPv3 compared to non-neoplastic samples. The 14-3-3 proteins comprise a large family of highly conserved phosphoserine/threonine-binding proteins related to intracellular signaling, apoptosis signal transduction, and cell cycle regulatory pathways, and being also negative regulators of cell death and cellular senescence (van Hemert et al., 2001). Furthermore, their aberrations are involved in cellular transformation and tumorigenesis, due to their role as oncoproteins and tumor suppressor proteins regulators (Morrison, 2009; Pennington et al., 2018). Interestingly, similarly to what observed in OaPV3-positive SCC, 14-3-3 zeta protein increases in high-risk human papillomavirus (HPV)-related cervical cancer, providing further evidence of the relationship between PVs and this family of phosphoserine/threonine-binding proteins (Boon et al., 2013). Considering the specific interaction of the 14-3-3 zeta protein with the phosphorylated PDZ binding motif (PBM) of the E6 viral protein reported in cervical cancer, it seems plausible that the higher abundance of 14-3-3 proteins in OaPV3-positive SCCs might be exclusively related to the viral presence and that it may contribute to maintaining high levels of OaPV3 E6 protein (Boon et al., 2013). Future studies involving the dissection of the role of E6 and of its possible relation and effects on 14-3-3 activity, as well as the 14-3-3 downstream pathway including, for example, the AKT and P53 pathway, should provide fascinating insights into the function of the E6 OaPV3 oncoprotein, considering also the unsolved p53 deregulation in ovine SCC cell proliferation (Tore et al., 2019).

Among the proteins decreased in OaPV3-positive SCCs when compared with the non-neoplastic tissue we found filaggrin 2, a protein involved in maintaining cell-cell adhesion and in the protection against UVB light, and transgelin-2, a protein that regulates actin cytoskeleton through actin binding and involved in cytoskeletal remodelling. Both proteins have been linked to human HPV-related cancer (Skaaby et al., 2014; Meng et al., 2017; Yang et al., 2019). Of interest is the observed overall decrease of galectins, including galectin-3, a β galactoside-binding protein, involved in tumor growth, progression, and metastasis, and considered a potential target to prevent

cancer metastasis (Ahmed et al., 2015). Similar to what observed in OaPV3-positive SCC, a decrease in galectin-3 was reported in human squamous and basal cell carcinomas (Kapucuoglu et al., 20019).

Among the 17 proteins significantly higher in OaPV3-positive SCCs when compared to OaPV3-negative SCCs, prosaposin, a lysosomal compartmental protein involved in catabolism of sphingolipids with small sugar chains, has been validated as oesophageal squamous cell carcinoma biomarker (Pawar et al., 2011).

Another interesting observation in the comparison of OaPV3-positive SCCs *vs* OaPV3-negative SCCs was the decreased abundance of proteins involved in epithelial cell differentiation and tissue development, such as type I and II cytokeratins (CKs), including CK 3, CK 6 and 15. This finding could be related to viral infection. Indeed, in our study, the markers for epidermal differentiation CK 3 and CK 6 were less abundant in OaPV3-positive SCC and more abundant in OaPV3-negative SCC, similarly to what reported in human cutaneous squamous cell carcinomas (Moll et al., 2008; Mommers et al., 2000). Nevertheless, *in vitro* studies have shown that the E1^E4 PV proteins are able to specifically bind CKs by a DEAD-box protein-mediated interaction, inducing the collapse of the cell cytoskeletal network (Raj et al., 2004). Likewise, our results support the deregulation of CK 6 induced by viral infection, and suggest an active role of OaPV3 in tissue development and epithelial cell differentiation.

Conversely, the increase in abundance of CK 13, a marker of epithelial differentiation for non-keratinizing epithelium such as the esophagus, appeared ambiguous considering also the observed decreased in the other proteins involved in epithelial cell differentiation and tissue development, as galectin-7 and transgelin-2 (Lam et al., 1995). This finding appears of interest since no altered levels of CK 13 were observed in OaPV3-negative SCC and in non-neoplastic tissues compared to OaPV3-positive SCC samples, suggesting that the increased abundance of this protein might be tightly related to viral infection. Interestingly, Hudson and co-workers reported overexpression of this protein in human cutaneous SCC (Hudson et al., 2010). Our hypothesis is

355 further reinforced by the IHC results, with a strong (60% of cases) and diffuse expression of CK 13
356 in OaPV3-positive malignant squamous cells, while no signal was detected in 100% of non-
357 neoplastic tissue and in most (80%) of OaPV3-negative SCC.

358 Nevertheless, our data conflicted with previous reports showing the ability of HPV 16
359 E1^E4 to bind CKs, inducing the collapse of the cell cytoskeletal network (Raj et al., 2004).
360 Overall, it seems conceivable that the decrease in CK 6 and CK 3 may activate the well-known
361 mechanism of cytokeratins compensation in which group I CK 13 is expressed in order to
362 compensate the absence of group II CKs (CK 6 and 3) (Kanaji et al., 2007). In particular, type I and
363 type II CKs have been shown to form obligate 1:1 heteropolymers, suggesting that dynamic
364 changes must occur in their expression levels, particularly when one CK is suppressed.

365 A limitation of this study could be related to sampling size and storage conditions. In
366 particular, a larger number of samples need to be systematically analyzed in order to make and
367 further validate general assumptions. Moreover, storage conditions could have nuanced the
368 proteomic features of virus-induced SCC. However, the storage condition used in this study
369 (freezing at -80°C immediately after sampling) is commonly used in proteomics studies (Tanca et
370 al., 2012). In addition, since both negative and positive samples underwent the same storage
371 process, we hypothesize that the differential proteomic results are reliable and are significantly
372 descriptive of the differences among OaPV3 positive, OaPV3 negative SCC, and non-SCC tissues.
373

374 **Conclusions**

375 To the best of our knowledge, this is the first study applying a comprehensive proteomic
376 approach for investigating the deregulation of proteins related to viral infection in one of the most
377 common ovine tumors, SCC. The altered biological processes as well as the SCC associated-
378 reactome might be related to viral pathogenesis pathways, suggesting that OaPV3 can represent a
379 driving force in neoplastic transformation, as proposed for several papillomavirus-related tumors.

The identification of altered molecular pathways involved in cell cycle and apoptosis, frequently reported in the literature as related to viral activity, envisages a specific virus-host interaction in which OaPV3 may favor malignant transformation. Considered together, our findings support a role of OaPV3 in the progression of cutaneous squamous cell carcinomas and recognized CK 13 as a promising putative biomarker of OaPV3 infection in ovine cutaneous SCCs, especially useful when the virus is undetectable in the tumor, and considering that OaPV3 specific antibodies suitable for IHC have not yet been developed.

Declaration of conflicting interests

The authors declared no potential conflicts of interest with respect to the research, authorship, and/or publication of this article.

Acknowledgments

The authors thank Dr. Marina Antonella Sanna for her support in the pathological specimen handling. This research was supported by the University of Sassari (Fondo di Ateneo per la Ricerca 2019 - Far2019Pirino – Far2019Burrai)

Appendix A: Supplementary material

Supplementary data associated with this article can be found, in the online version, at doi:

References

Addis, M.F., Pisanu, S., Ghisaura, S., Pagnozzi, D., Marogna, G., Tanca, A., Biosa, G., Cacciotto, C., Alberti, A., Pittau, M., et al., 2011. Proteomics and Pathway Analyses of the Milk Fat Globule in Sheep Naturally Infected by Mycoplasma agalactiae Provide Indications of the In Vivo Response of the Mammary Epithelium to Bacterial Infection. Infection and Immunity 79, 3833-3845.

Addis, M.F., Pisanu, S., Marogna, G., Cubeddu, T., Pagnozzi, D., Cacciotto, C., Campesi, F., Schianchi, G., Rocca, S., Uzzau, S., 2013. Production and release of antimicrobial and immune

defense proteins by mammary epithelial cells following Streptococcus uberis infection of sheep. Infect Immun 81, 3182-3197.

Ahmed, A.F., Hassanein, K.M.A., 2012. Ovine and caprine cutaneous and ocular neoplasms. Small Ruminant Res 106, 189-200.

Ahmed, H., AlSadek, D.M.M., 2015. Galectin-3 as a Potential Target to Prevent Cancer Metastasis. Clin Med Insights-On 9, 113-121.

Alberti, A., Pirino, S., Pintore, F., Addis, M.F., Chessa, B., Cacciotto, C., Cubeddu, T., Anfossi, A., Benenati, G., Coradduzza, E.,et al., 2010. Ovis aries Papillomavirus 3: A prototype of a novel genus in the family Papillomaviridae associated with ovine squamous cell carcinoma. Virology 407, 352-359.

Banco, B., Antuofermo, E., Borzacchiello, G., Cossu-Rocca, P., Grieco, V., 2011. Canine ovarian tumors: an immunohistochemical study with HBME-1 antibody. J Vet Diagn Invest 23, 977-981.

Boon, S.S., Banks, L., 2013. High-Risk Human Papillomavirus E6 Oncoproteins Interact with 14-3-3 zeta in a PDZ Binding Motif-Dependent Manner. J Virol 87, 1586-1595.

Burrai, G.P., Tanca, A., De Miglio, M.R., Abbondio, M., Pisanu, S., Polinas, M., Pirino, S., Mohammed, S.I., Uzzau, S., Addis, M.F., Antuofermo, E., 2015. Investigation of HER2 expression in canine mammary tumors by antibody-based, transcriptomic and mass spectrometry analysis: is the dog a suitable animal model for human breast cancer? Tumor Biol 36, 9083-9091.

Calmon, M.F., Mota, M.T.D., Babeto, E., Candido, N.M., Girol, A.P., Mendiburu, C.F., Bonilha, J.L., Silvestre, R.V.D., Rosa, B.M., Thome, J.A.,et al., 2013. Overexpression of ANXA1 in Penile Carcinomas Positive for High-Risk HPVs. Plos One 8.

Ceciliani, F., Eckersall, D., Burchmore, R., Lecchi, C., 2014. Proteomics in Veterinary Medicine Applications and Trends in Disease Pathogenesis and Diagnostics. Veterinary Pathology 51, 351-362.

Croce, M.V., Price, M.R., Segal-Eiras, A., 2001. Association of a alpha1 acidic glycoprotein and squamous cell carcinoma of the head and neck. Pathol Oncol Res 7, 111-117.

Gil da Costa, R.M., Peleteiro, M.C., Pires, M.A., DiMaio, D., 2017. An Update on Canine, Feline and Bovine Papillomaviruses. Transbound Emerg Dis 64, 1371-1379.

de Villiers, E.M., 2013. Cross-roads in the classification of papillomaviruses. Virology 445, 2-10.

Fouad, Y.A., Aanei, C., 2017. Revisiting the hallmarks of cancer. Am J Cancer Res 7, 1016-1036.

Fridman, J.S., Lowe, S.W., 2003. Control of apoptosis by p53. Oncogene 22, 9030-9040.

Fuentes-Gonzalez, A.M., Contreras-Paredes, A., Manzo-Merino, J., Lizano, M., 2013. The modulation of apoptosis by oncogenic viruses. Virol J 10, 182.

Ghisaura, S., Pagnozzi, D., Melis, R., Biosa, G., Slawski, H., Uzzau, S., Anedda, R., Addis, M.F., 2019. Liver proteomics of gilthead sea bream (Sparus aurata) exposed to cold stress. J Therm Biol 82, 234-241.

Gibbons, P.M., Lamb, L., Mansell, J., 2015. Presentation, treatment, and outcome of squamous cell carcinoma in the perineal region of 9 goats. Can Vet J 56, 1043-1047.

Goldschmidt, M.H., Goldschmidt, K.H., 2017. Epithelial and Melanocytic Tumors of the Skin. In: Meuten DJ, ed. Tumors in domestic animals, 5th edition. Wiley Blackwell, USA.

Hudson, L.G., Gale, J.M., Padilla, R.S., Pickett, G., Alexander, B.E., Wang, J., Kusewitt, D.F., 2010. Microarray analysis of cutaneous squamous cell carcinomas reveals enhanced expression of epidermal differentiation complex genes. Mol Carcinog 49, 619-629.

Kall, L., Canterbury, J.D., Weston, J., Noble, W.S., MacCoss, M.J., 2007. Semi-supervised learning for peptide identification from shotgun proteomics datasets. Nat Methods 4, 923-925.

Kanaji, N., Bandoh, S., Fujita, J., Ishii, T., Ishida, T., Kubo, A., 2007. Compensation of type I and type II cytokeratin pools in lung cancer. Lung Cancer-J Iaslc 55, 295-302.

Kapucuoglu, N., Basak, P.Y., Bircan, S., Sert, S., Akkaya, V.B., 2009. Immunohistochemical galectin-3 expression in non-melanoma skin cancers. Pathol Res Pract 205, 97-103.

Kurihara-Shimomura, M., Sasahira, T., Nakashima, C., Kuniyasu, H., Shimomura, H., Kirita, T., 2018. The Multifarious Functions of Pyruvate Kinase M2 in Oral Cancer Cells. Int J Mol Sci 19.

Lam, K.Y., Loke, S.L., Shen, X.C., Ma, L.T., 1995. Cytokeratin expression in non-neoplastic oesophageal epithelium and squamous cell carcinoma of the oesophagus. Virchows Arch 426, 345-349.

Lange, C.E., Favrot, C., 2011. Canine papillomaviruses. Vet Clin North Am Small Anim Pract 41, 1183-1195.

Lippolis, R., De Angelis, M., 2016.Proteomics and human diseases. J Proteomics Bioinform 9: 063-074.

Lecis, R., Mucedda, M., Pidinchedda, E., Zobba, R., Pittau, M., Alberti, A., 2020. Genomic characterization of a novel bat-associated Circovirus detected in European Miniopterus schreibersii bats. Virus Genes 56, 325-328.

Mabert, K., Cojoc, M., Peitzsch, C., Kurth, I., Souchelnytskyi, S., Dubrovska, A., 2014. Cancer biomarker discovery: Current status and future perspectives. Int J Radiat Biol 90, 659-677.

Meng, T., Liu, L.C., Hao, R.F., Chen, S.Y., Dong, Y.L., 2017. Transgelin-2: A potential oncogenic factor. Tumor Biol 39.

Moll, R., Divo, M., Langbein, L., 2008. The human keratins: biology and pathology. Histochem Cell Biol 129, 705-733.

Mommers, J.M., van Rossum, M.M., van Erp, P.E.J., van de Kerkhof, P.C.M., 2000. Changes in keratin 6 and keratin 10 (co-)expression in lesional and symptomless skin of spreading psoriasis. Dermatology 201, 15-20.

Morrison, D.K., 2009. The 14-3-3 proteins: integrators of diverse signaling cues that impact cell fate and cancer development. Trends Cell Biol 19, 16-23.

Munday, J.S., Kiupel, M., 2010. Papillomavirus-Associated Cutaneous Neoplasia in Mammals. Veterinary Pathology 47, 254-264.

Munday, J.S., 2014. Bovine and Human Papillomaviruses: A Comparative Review. Veterinary Pathology 51, 1063-1075.

Old, W.M., Meyer-Arendt, K., Aveline-Wolf, L., Pierce, K.G., Mendoza, A., Sevinsky, J.R., Resing, K.A., Ahn, N.G., 2005. Comparison of label-free methods for quantifying human proteins by shotgun proteomics. Mol Cell Proteomics 4, 1487-1502.

Pawar, H., Kashyap, M.K., Sahasrabuddhe, N.A., Renuse, S., Harsha, H.C., Kumar, P., Sharma, J., Kandasamy, K., Marimuthu, A., Nair, B., et al., 2011. Quantitative tissue proteomics of esophageal squamous cell carcinoma for novel biomarker discovery. Cancer Biol Ther 12, 510-522.

Pennington, K.L., Chan, T.Y., Torres, M.P., Andersen, J.L., 2018. The dynamic and stress-adaptive signaling hub of 14-3-3: emerging mechanisms of regulation and context-dependent protein-protein interactions. Oncogene 37, 5587-5604.

Pham, T.V., Piersma, S.R., Warmoes, M., Jimenez, C.R., 2010. On the beta-binomial model for analysis of spectral count data in label-free tandem mass spectrometry-based proteomics. Bioinformatics 26, 363-369.

Pisanu, S., Cubeddu, T., Cacciotto, C., Pilicchi, Y., Pagnozzi, D., Uzzau, S., Rocca, S., Addis, M.F., 2018. Characterization of paucibacillary ileal lesions in sheep with subclinical active infection by Mycobacterium avium subsp paratuberculosis. Vet Res 49.

Pisanu, S., Ghisaura, S., Pagnozzi, D., Biosa, G., Tanca, A., Roggio, T., Uzzau, S., Addis, M.F., 2011. The sheep milk fat globule membrane proteome. J Proteomics 74, 350-358.

Raj, K., Berguerand, S., Southern, S., Doorbar, J., Beard, P., 2004. E1 empty set E4 protein of human papillomavirus type 16 associates with mitochondria. J Virol 78, 7199-7207.

Rector, A., Van Ranst, M., 2013. Animal papillomaviruses. Virology 445, 213-223.

Sardon, D., Blundell, R., Burrai, G.P., Alberti, A., Tore, G., Passino, E.S., Antuofermo, E., 2015. Absence of canine papillomavirus sequences in canine mammary tumours. J Comp Pathol 152, 172-176.

Scheffner, M., Werness, B.A., Huibregtse, J.M., Levine, A.J., Howley, P.M., 1990. The E6 oncoprotein encoded by human papillomavirus types 16 and 18 promotes the degradation of p53. Cell 63, 1129-1136.

Shaul, M.E., Fridlender, Z.G., 2019. Tumour-associated neutrophils in patients with cancer. Nat Rev Clin Oncol 16, 601-620.

Skaaby, T., Husemoen, L.L., Jorgensen, T., Johansen, J.D., Menne, T., Szecsi, P.B., Stender, S., Bager, P., Thyssen, J.P., Linneberg, A., 2014. Associations of filaggrin gene loss-of-function variants and human papillomavirus-related cancer and pre-cancer in Danish adults. Plos One 9, e99437.

Srivastava, A., Creek, D.J., 2019. Discovery and Validation of Clinical Biomarkers of Cancer: A Review Combining Metabolomics and Proteomics. Proteomics 19, e1700448.

Szklarczyk, D., Franceschini, A., Wyder, S., Forslund, K., Heller, D., Huerta-Cepas, J., Simonovic, M., Roth, A., Santos, A., Tsafou, K.P., et al., 2015. STRING v10: protein-protein interaction networks, integrated over the tree of life. Nucleic Acids Res 43, D447-452.

Tanca, A., Pagnozzi, D., Burrai, G.P., Polinas, M., Uzzau, S., Antuofermo, E., Addis, M.F., 2012. Comparability of differential proteomics data generated from paired archival fresh-frozen and formalin-fixed samples by GeLC-MS/MS and spectral counting. J Proteomics 77, 561-576.

Tanca, A., Pisanu, S., Biosa, G., Pagnozzi, D., Antuofermo, E., Burrai, G.P., Canzonieri, V., Cossu-Rocca, P., De Re, V., Eccher, A., et al., 2013. Application of 2D-DIGE to formalin-fixed diseased tissue samples from hospital repositories: results from four case studies. Proteomics Clin Appl 7, 252-263.

The, M., MacCoss, M.J., Noble, W.S., Kall, L., 2016. Fast and Accurate Protein False Discovery Rates on Large-Scale Proteomics Data Sets with Percolator 3.0. J Am Soc Mass Spectrom 27, 1719-1727.

Tore, G., Cacciotto, C., Anfossi, A.G., Dore, G.M., Antuofermo, E., Scagliarini, A., Burrai, G.P., Pau, S., Zedda, M.T., Masala, G., et al., 2017. Host cell tropism, genome characterization, and evolutionary features of OaPV4, a novel Deltapapillomavirus identified in sheep fibropapilloma. Vet Microbiol 204, 151-158.

Tore, G., Dore, G.M., Cacciotto, C., Accardi, R., Anfossi, A.G., Bogliolo, L., Pittau, M., Pirino, S., Cubeddu, T., Tommasino, M., et al., 2019. Transforming properties of ovine papillomaviruses E6 and E7 oncogenes. Vet Microbiol 230, 14-22.

van Hemert, M.J., Steensma, H.Y., van Heusden, G.P., 2001. 14-3-3 proteins: key regulators of cell division, signalling and apoptosis. Bioessays 23, 936-946.

Vitiello, V., Burrai, G.P., Agus, M., Anfossi, A.G., Alberti, A., Antuofermo, E., Rocca, S., Cubeddu, T., Pirino, S., 2017. Ovis aries Papillomavirus 3 in Ovine Cutaneous Squamous Cell Carcinoma. Vet Pathol 54, 775-782.

Wisniewski, J.R., Zougman, A., Nagaraj, N., Mann, M., 2009. Universal sample preparation method for proteome analysis. Nat Methods 6, 359-362.

Yang, R., Klimentova, J., Gockel-Krzikalla, E., Ly, R., Gmelin, N., Hotz-Wagenblatt, A., Rehulkova, H., Stulik, J., Rosl, F., Niebler, M., 2019. Combined Transcriptome and Proteome Analysis of Immortalized Human Keratinocytes Expressing Human Papillomavirus 16 (HPV16) Oncogenes Reveals Novel Key Factors and Networks in HPV-Induced Carcinogenesis. mSphere 4.

612 Zybailov, B., Mosley, A.L., Sardiu, M.E., Coleman, M.K., Florens, L., Washburn, M.P., 2006.
613 Statistical analysis of membrane proteome expression changes in Saccharomyces cerevisiae. J
614 Proteome Res 5, 2339-2347.

615 **Table 1**

616 Differential proteins and their biological function in OaPV3-positive SCC vs OaPV3-negative SCC (OaPV3 vs SCC), OaPV3-positive SCC vs non-
617 SCC (OaPV3 vs N), and OaPV3-negative SCC vs non-SCC (SCC vs N), respectively. Values are expressed in relative spectral counts (R_{SC}).
618 Differences in abundance are reported as fold changes in the respective sample comparisons. Statistically significant differential values are in bold:
619 Rsc ≤ −1.5 or ≥ 1.5, beta-binomial test P ≤ 0.05. Protein identities obtained upon BLAST search. Response to stress (RS), regulation of apoptotic
620 signaling pathway (RASP), negative regulation of apoptotic process (NRAP), negative regulation of cell death (NRCD), tissue development (TD),
621 epithelial cell differentiation (ECD), extracellular matrix disassembly (EMD), extracellular matrix organization (EMO), glycosaminoglycan
622 catabolic process (GCP)

Accession	Gene Nane	Protein name	OaPV3 vs SCC	OaPV3 vs N	SCC vs N	Biological process								
						RS	RASP	NRAP	NRCD	TD	ECD	EMD	EMO	GCP
Q99877	HIST1H2BN	Histone H2B type 1-N	**3.37**	1.48	**-1.91**									
P13796	LCP1	Plastin-2	**3.33**	0.42	**-2.94**							*	*	
P13646	KRT13	Keratin, type I cytoskeletal 13	**3.20**	**2.54**	-	*								
P69905	HBA1	I alpha globin	**2.64**	**1.57**	-1.09									
P07602	PSAP	Prosaposin	**2.61**	1.10	-	*			*	*	*			
Q8IVF2	AHNAK2	Protein AHNAK2	**2.47**	**1.81**	-									
P22309	UGT1A1	UDP-glucuronosyltransferase 1-1	**2.47**	1.46	-	*								
O75594	PGLYRP1	Peptidoglycan recognition protein 1	**2.40**	-0.25	-	*								*
Q04917	YWHAH	14-3-3 protein theta	**2.38**	**3.36**	-		*							
O14950	MYL12B	Myosin regulatory light chain 12B	**2.26**	**2.47**	-0.89									
P08238	HSP90AB1	Heat shock protein HSP 90-beta	**1.95**	1.28	-			*	*				*	
P00558	PGK1	Phosphoglycerate kinase	**1.95**	-0.24	**-2.21**					*	*			
P36871	PGM1	Phosphoglucomutase-1	**1.80**	1.48	-									

Q09666	AHNAK	Neuroblast differentiation-associated protein AHNAK	**1.75**	1.16	-0.62												
P29034	S100A2	Protein S100-A2	**1.69**	1.40	-												
P49913	CAMP	Cathelicidin antimicrobial peptide	**1.59**	-0.72	-0.31	*							*				
P68871	HBB	Hemoglobin subunit beta	**1.53**	**1.57**	0.01	*											
P37802	TAGLN2	Transgelin-2	1.40	**1.68**	0.26						*	*					
P09211	GSTP1	Glutathione S-transferase P	1.36	**2.18**	0.80	*	*	*	*								
P14618	PKM	Pyruvate kinase	1.31	**2.62**	1.29						*						
B9A064	IGLL5	Immunoglobulin lambda-like polypeptide 5	1.29	**1.83**	0.51	*											
P50454	SERPINH1	Serpin H1	1.09	**1.78**	0.67	*					*			*			
P14174	MIF	Macrophage migration inhibitory factor	0.95	-0.75	**-1.73**	*	*	*	*								
P08758	ANXA5	Annexin	0.84	**2.41**	**1.55**	*		*	*								
P63104	YWHAZ	14-3-3 protein zeta/delta	0.75	**1.93**	1.16	*	*	*	*								
P00441	SOD1	Superoxide dismutase [Cu-Zn]	0.69	-0.83	**-1.54**	*	*	*	*		*	*					
P10909	CLU	Clusterin	0.69	-2.05	**-2.76**	*	*	*	*								
P68371	TUBB4B	Tubulin beta-4B chain	0.59	3.15	**2.53**	*											
P02763	ORM1	Alpha-1-acid glycoprotein	0.14	**1.95**	**1.78**	*											
P09493	TPM1	Tropomyosin alpha-1 chain	0.07	**-1.62**	**-1.72**	*					*						
P01861	IGHG4	Ig gamma-4 chain C region	-0.02	1.82	**1.81**												
P07585	DCN	Decorin	-0.34	**-1.64**	-1.32	*					*		*	*	*		
P12111	COL6A3	Collagen alpha-3(VI) chain	-0.46	**-1.71**	-1.27								*	*			
P68104	EEF1A1	Elongation factor 1-alpha 1	-0.48	1.22	**1.68**												
P35754	GLRX	Glutaredoxin-1	-0.78	**-2.12**	-1.36						*						
P18206	VCL	Vinculin	-0.83	**-1.96**	-1.15	*											
P12109	COL6A1	Collagen alpha-1(VI) chain	-0.96	**-2.45**	-1.51						*		*	*			
P02765	AHSG	Alpha-2-HS-glycoprotein	-0.97	**-1.90**	-0.96	*							*				
P07951	TPM2	Tropomyosin beta chain	-1.06	**-2.35**	-1.32												
Q9BXN1	ASPN	Asporin	-1.31	**-2.67**	-1.38						*						
P20774	OGN	Mimecan	**-1.55**	**-3.43**	**-1.90**											*	
P01834	IGKC	Ig kappa chain C region	**-1.70**	0.00	0.74												
P04264	KRT1	Keratin, type II cytoskeletal 1	**-1.86**	**-2.47**	-0.63	*					*						
P51888	PRELP	Prolargin	-1.92	**-2.55**	-0.65											*	

P47929	LGALS7	Galectin-7	**-2.00**	**-2.36**	-0.38				
A2N2W8	VL6	VL6 protein	**-2.00**	0.00	0.77				
P04264	KRT1	Keratin, type II cytoskeletal 1	**-2.27**	**-2.86**	-0.61	*		*	
Q01995	TAGLN	Transgelin	**-2.34**	**-3.05**	-0.73			*	*
P62736	ACTA2	Actin, aortic smooth muscle	**-3.67**	**-4.15**	-0.51			*	*
P19012	KRT15	Keratin, type I cytoskeletal 15	**-4.77**	0.00	2.77	*		*	
P12035	KRT3	Keratin, type II cytoskeletal 3	**-4.88**	0.00	**2.61**			*	*
P48668	KRT6C	Keratin, type II cytoskeletal 6C	**-5.89**	0.00	**5.27**				

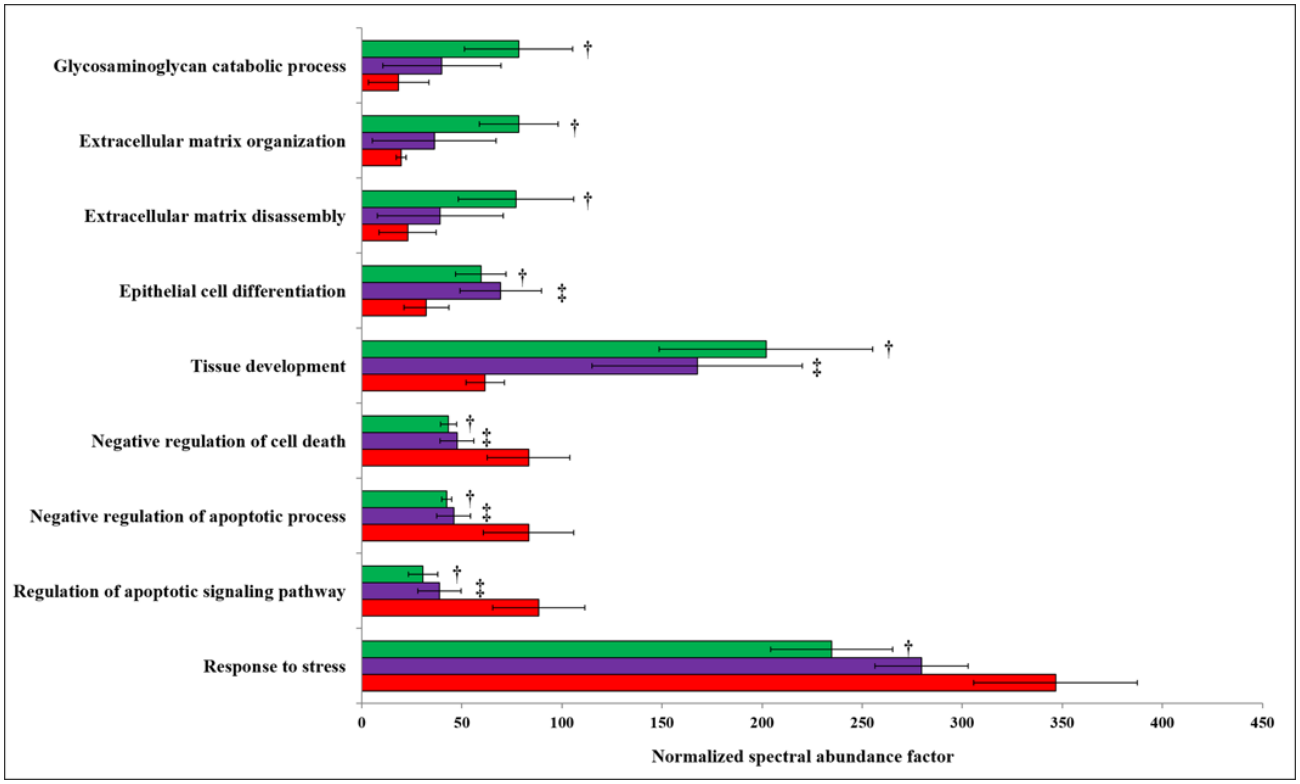

Fig. 1. Comparative abundance of biological processes related to the differential proteins observed when comparing OaPV3-positive SCCs (red), OaPV3-negative SCCs (violet) and non-SCC samples (green). Data are shown as mean ± s.d. from n=3 samples. † $P \leq 0.05$, *t*-test comparing OaPV3-positive SCCs to non-SCC samples. ‡ $P \leq 0.05$, *t*-test comparing OaPV3-positive SCCs to OaPV3-negative SCCs.

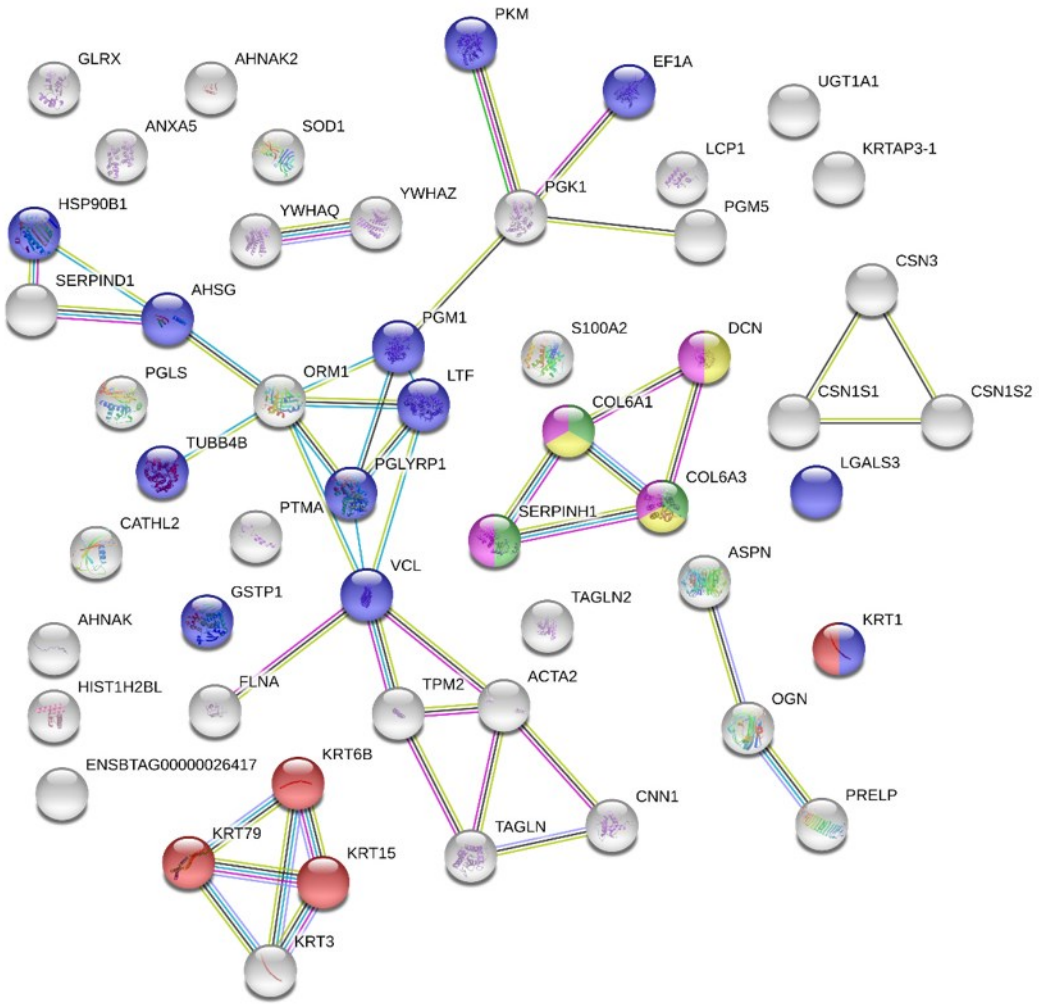

631

632 Fig. 2. Reactome network according to STRING. Proteins associated with Innate Immune System,
633 Formation of the cornified envelope, Collagen biosynthesis and modifying enzymes, Degradation of
634 the extracellular matrix, and Extracellular matrix organization are indicated in purple, red, green,
635 yellow and pink, respectively. Seven different colored lines link nodes and represent seven types of
636 evidence used in predicting associations. Green lines: neighborhood evidence; red lines: presence of
637 fusion evidence; blue lines: co-occurrence evidence; black lines: co-expression evidence; purple
638 lines: experimental evidence; light blue lines: database evidence; yellow lines: text-mining
639 evidence.

640

641

642 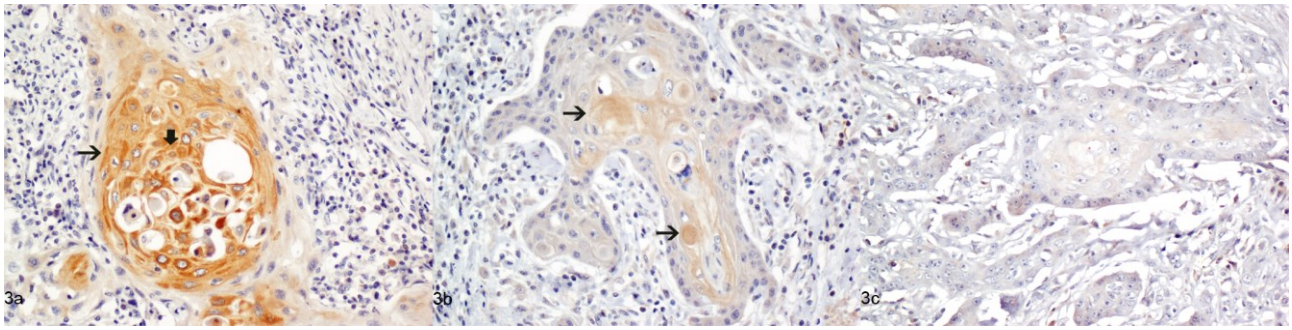

643 Fig. 3. Immunohistochemistry of cytokeratin 13. Strong (3a) immunoreactivity detected in the
644 intermediate (thin arrow) and superficial layers (thick arrow) of OaPV3-positive malignant
645 squamous cells. Weak (3b) immunosignal observed in intermediate layers (thin arrow) of OaPV3-
646 positive malignant squamous cells. No immunostain (3c) was detected in OaPV3-negative
647 squamous cell carcinoma. Bar 10 µm.